Published in final edited form as:
Circ Cardiovasc Imaging. 2010 November 1; 3(6): 710–717. doi:10.1161/CIRCIMAGING.110.959098.

Early Impairment of Transmural Principal Strains in the Left Ventricle Wall Following Short-Term, High Fat Feeding of Mice Predisposed to Cardiac Steatosis

Janusz H. Hankiewicz, Ph.D., **Natasha H. Banke, Ph.D.**, **Mariam Farjah, Ph.D.**, and **E. Douglas Lewandowski, Ph.D.**
Program in Integrative Cardiac Metabolism, Center for Cardiovascular Research, University of Illinois at Chicago, College of Medicine, Chicago, IL, USA

Abstract

Background—Myocardial lipid accumulation precedes some cardiomyopathies, but little is known of concurrent effects on ventricular mechanics. We tested the hypothesis that intramyocardial lipid accumulation, during short term high fat diet (HFD), affects 2-D strains in the heart. We examined hearts of nontransgenic (NTG) mice and transgenic mice predisposed to elevated triacylglyceride (TAG) storage linked to low-level overexpression of PPARα.

Methods and Results—Myocardial lipid and transmural, principal strains E1 and E2 were determined *in vivo* with ^{1}H MRS/MRI before and after 2 weeks of HFD in both PPARα and NTG littermate mice. Baseline lipid was elevated in PPARα over NTG. HFD increased mobile lipid by 174% in NTG ($P<0.05$) and 79% in PPARα ($P<0.05$). After HFD, lipid and TAG were higher in PPARα versus NTG, by 63% and 81%, respectively. However, TAG in PPARα after HFD was similar to TAG in PPARα on regular diet, suggesting that the MRS signal from lipid is not exclusive to TAG. Only at the highest lipid contents, achieved in PPARα, were strains affected. Endocardial strain was most compromised, with a negative correlation to lipid ($P<0.05$),

Conclusions—Short term high fat diet elevated myocardial lipid measures via MRS which became dissociated from TAG content in hearts predisposed to cardiac steatosis. The increased lipid was associated with concurrent, transmural reductions in E1 and E2 strains across the LV wall. Strains were attenuated at the highest levels of lipid accumulation suggesting a threshold response. Thus, 2-D strains are impaired early and without LV diastolic dysfunction due to cardiac steatosis.

Keywords

cardiomyopathy; lipids; magnetic resonance imaging; spectroscopy

INTRODUCTION

The role of lipid content in myocardium is an increasingly recognized component in the pathogenesis of heart failure, yet the mechanisms linking these phenomena remain elusive. The over storage of lipid in human myocardium, or cardiac steatosis, is an early manifestation of type II diabetes that precedes development of diabetic cardiomyopathy[1]. In

Correspondence to: E. Douglas Lewandowski, Ph.D., Department of Physiology and Biophysics, MC901, UIC College of Medicine, 835 South Wolcott Avenue, Chicago, IL 60612, USA, 312-413-7261, (Fax) 312-996-2870, dougl@uic.edu.

DISCLOSURES
None.

animal models, evidence exists for direct detrimental effects of lipotoxicity resulting from altered fatty acid metabolism in the heart [2–4], while the mere accumulation of myocardial triglycerides has been related to the eventual development of cardiac dysfunction[5–8]. While such findings link elevated myocardial lipid content to cardiomyopathy, the influence of high fat diet on myocardial lipid content and the potential for consequential, short-term changes in cardiac mechanics is not clear. The potential exists for both the biochemical action of altered acyl intermediates and the mechanical constraints imposed by lipid infiltration to affect contractility[9–11]. Therefore, the current study examines the short-term effects of high fat diet (HFD) on mobile lipid content in the myocardium and principal 2-dimensional (2-D) strains (E1, E2) in the *in vivo* mouse heart.

With the first combined measures of lipid content, via localized ^{1}H MRS, with high resolution, cardiac tagged MRI of transmural strains in the *in vivo* mouse heart in a single scanning period, we examined the longitudinal effects of a short term, high fat diet on both intramyocardial lipid and the 2-D principal strains in the epi- and endocardial layers of the left ventricular (LV) wall. The initial development of high resolution cardiac MRI tagging grids, of 0.33 mm, in our laboratory has enabled different responses of 2-D strains in endocardial and epicardial layers to be distinguished[12]. In studying the link between cardiac lipid content and 2-D strain, we examined the responses of both normal mice and a transgenic mouse model (MHC-PPARα) of elevated myocardial triacylglyceride due to chronic, low-level, cardiac-specific overexpression of the peroxisome proliferator activated receptor alpha (PPARα)[13].

Previous studies of hearts from this novel transgenic model have shown global indices of LV dysfunction following more prolonged exposure to high fat diet than applied in the current in vivo study of 2-D strains across the LV wall[14]. The current approach tested the hypothesis that intramyocardial lipid accumulation, due to short-term high fat diet, induces early, transmural changes in positive and negative 2-D strains in the LV wall, prior to evidence of altered diastolic function. Additionally, the protocol enabled distinction between changes in the mobile lipid pool, as detected by ^{1}H MRS, and the triacylglyceride pool, from assays of tissue samples. The findings provide new insights into the LV wall mechanics of the hearts exposed to high fat diets with potential for lipid accumulation, and suggest a stepwise effect, or threshold in myocardial lipid levels in contributing to contractile dysfunction.

METHODS

Animal model

Experiments were performed on 5 month old mice with low-level cardiac-specific, overexpression of PPARα in the heart, driven by the alpha myosin heavy chain promoter (MHC-PPARα, line 404-4) and age-matched, non-transgenic littermates (NTG): NTG, n=8; MHC-PPARα, n=8. Separate groups of mice (NTG, n=4; MHC-PPARα, n=4) were sacrificed to determine baseline myocardial TAG content prior to the protocols. Additional NTG (n=3) and MHC-PPARα mice (n=3) were studied before and after 2 weeks of regular chow diet (RCD) as additional controls. No gender differences in the measured parameters occurred among either transgenic or NTG mice at any point in the protocols. This cardiac specific, low overexpressing line of MHC-PPARα mice, line 404-4, has been described earlier[14]. Mice were housed under controlled temperature, humidity and light and provided *ad libitum* with normal chow (Harlan Teklad, Madison, WI, USA. Diet 7012 Teklad LM-485: fat 17%, carbohydrate 58%, protein 25%) and water. For HFD studies, pre-diet analyses were performed and the regular chow was replaced with high fat chow (Harlan Teklad, Madison, WI, USA. Diet # TD 97268: fat 43%, carbohydrate 38%, protein 19%) for

a two week period. All experimental procedures were approved by the UIC Animal Care and Use Committee.

Anesthesia was initiated with 5% of Isoflurane (Minard Inc, Bethlehem, PA) in 100% medical grade Oxygen from a flow vaporizer (Surgivet, Waukesha, Wisconsin, USA) and maintained with 1.0–1.2 % Isoflurane in 2L/min flow of 100% medical grade Oxygen, administered through a nose cone. After 3 minutes, mice were weighed and restrained, supine, in a dedicated cradle. Excess vapor was drawn by a gas evacuating system (Surgivet, Waukesha, Wisconsin, USA) through a charcoal filter (AM Bickford Inc, Wales Center, New York, USA). Body temperature was continuously monitored and maintained at 37°C.

For cardiac gating, subcutaneous ECG electrodes were inserted at the front right and rear left legs. Respiratory gating was achieved with a pneumatic pillow (Sims Graseby Ltd, Watford, UK). ECG, respiratory, and temperature signals were transferred through a fiber optic device to a PC compatible animal monitoring system (SA Instruments, Stony Brook, New York, USA).

MRI/MRS Acquisition

Imaging and localized spectroscopy was performed on a 600 MHz Bruker, Avance console (Bruker Biospin, Billerica, Massachusetts, USA) equipped with an actively shielded 14.1 T, 89 mm bore vertical magnet and 1000 mT/m, 110 μs rise time micro-imaging gradient system. Paravision 4.0 and corresponding Topspin 1.5 control programs were used to conduct MRI and MRS experiments. The restrained mouse with cradle was placed in an upright position in a linearly polarized 600 MHz birdcage resonator (inner diameter 26 mm and active length of 52mm). To avoid motion artifacts and assure reproducible volume localization for spectroscopy, all acquired images and spectra were cardiac-triggered and blanked during the inspiration.

The experimental protocol consisted of heart localization, cardiac tagging and localized spectroscopy. After positioning the mouse in the magnet, the heart was localized with a group of orthogonal and oblique images using fast gradient echo sequence FLASH (Fast Low Angle SHot). Depending on the heart and respiration rates, total experimental time was about 2 hours.

Cardiac tagging—For 2-D principal strain measurements, true, short axis tagged images were acquired with a high resolution grid (0.33 × 0.33 mm^2 in-plane dimension and less than 0.1 mm line thickness) using the modified DANTE sequence described previously[12]. The sequence saturates ^1H nuclei in two orthogonal planes, suppressing NMR signal during imaging. This suppression generates a visible dark square grid on images perpendicular to suppressed planes taken after tagging. The tagging grid decay is determined by tissue spin-lattice T_1 relaxation time and can be used to track tissue motion during myocardial contraction and expansion. Following the tagging grid generation at least 8 tagged images (TE= 1.9 ms, TR>300 ms, FOV=20 mm, slice thickness 1 mm, number of acquisitions NA = 4 and acquisition matrix 256×256) were acquired from end-diastole through end-systole up to rapid filling of the LV with a temporal resolution of 8 ms.

Localized cardiac MRS—Localized ^1H NMR spectroscopy (MRS) was performed with a modified cardiac triggering and respiratory blanked PRESS (Point RESolved Spectroscopy) sequence. To avoid contamination from pericardial fat, very small volumes of interest (VOI) of the size of 1×1×1 mm (1 μl) were selected within the septum[15–17] at midventricular from axial and sagittal scout images (Figure 1a). To match the MRS volume, location measurements of E1 and E2 were performed on the midventricular septum in both epi- and endo-cardium layers. Manual shimming was conducted with PRESS sequence without water

suppression on a larger VOI of 3×3×2 mm^3 covering the midventricular septum (TR>250ms). Line width (half height) of the unsuppressed proton signal of water peak ranged 50–90 Hz.

For MRS, the ECG R-wave triggered a CHESS (Chemical Shift Selective) water suppression train of three saturation, narrow-band hermite pulses (length = 21.6 ms, bandwidth = 250 Hz). Each saturation pulse was followed by gradients to destroy water transverse magnetization. Entire suppression time was 90 ms, and was shorter than the shortest recorded R-R period (95 ms). The next R peak in the ECG triggered the execution of voxel-selective stimulated echo sequence with 1 ms hermite pulses (BW = 5,400 Hz) to excite protons in a selected VOI at the end of diastole. Spoiling gradients followed excitation pulses to suppress unwanted signal components and determined an echo time (TE) of 11.5 ms.

The proton signal from water was determined from a brief unsuppressed PRESS experiment (TR > 500 ms, NA = 64) with a reproducibility within 7%. The carrier frequency was centered between the water and the methylene peaks. Water-suppressed (NA = 512) and unsuppressed (NA = 128) spectra were acquired from the same volume for quantitative comparison of lipid. Complex data points (1024) were acquired with 8 kHz receiver spectral width and TR>2,500 ms. Figure 1b shows representative *in vivo* spectra acquired from the midventricular septum of PPARα and NTG mice before and after HF diet.

Triacylglyceride assay

Following the post-diet protocol, mice were anesthetized (80mg/kg Ketamine and 12mg/kg Xylazine, i.p.), and hearts were excised and frozen in liquid nitrogen. Lipid extracts were obtained, and triacylglerides were quantified by colorimetric assay (Wako Pure Chemical Industries, Osaka, Japan) as previously described[18].

MRI/MRS data analysis

Tagged images were zero-filled to 512×512 at 0.039 mm/pixel and processed with Matlab (MathWorks, Natick, MA)[19]. For homogenous strain calculations, the reference frame was the image taken at end-diastole. Figure 2a and 2b show representative tagged images at end-diastole and end-systole obtained with a 0.33 mm tagging resolution with 3 grids resolved across the LV wall. Motion of the tagging grid required manual tracking. Deformed tagging square-like elements were divided into two adjacent triangles and the position of the centroids calculated[20]. Strains were calculated from relative displacement of coupled centroids of the epicardial and endocardial elements and endocardial, excluding mid-wall elements (Figure 2c and 2d). Maximum strain values were assigned as diastole-systole strain. Epicardial and endocardial contours of tagged images were used to determine percentage of wall thickening (%WT) in four segments of the mid LV wall (septal, lateral, anterior, and posterior) and LV internal diameter at diastole ($LVID_d$).

Time domain MRS signals were zero-filled to 16k, exponentially filtered, and following Fourier transformation, phase corrected. Chemical shifts were assigned relative to water at 4.7 ppm. For comparison of lipids, acyl-chain methylene signals were integrated and normalized to signal from unsuppressed water.

Statistical analysis

All statistics were performed using GraphPad Prism version 5.02 for Windows (GraphPad Software, San Diego, CA). Mean values between MHC-PPARα mice and wild-type NTG mice were compared using the unpaired Student's T-Test. Intergroup comparison of means was performed using ANOVA with a Bonferroni post-test. Intragroup comparisons of means

were performed using a Student's paired T-Test. The Person r was used for bivariate correlation analysis between lipids accumulation and strains, and between lipids accumulation and TAG content. All data are presented as means ± standard deviation, with statistical significance at <5% probability.

RESULTS

Animal Model

Heart rates in the anesthetized mice, situated in the imaging probe, were similar to previously reported, physiological rates ranging 400 – 634 bpm[21–23]. Body weight of NTG mice was unaffected by the two week high fat diet (prediet: 28.7±4.2 g, postdiet: 28.8±4.0 g), while mean body weight of MHC-PPARα mice increased by 5% (prediet: 24.9 ±2.5 g, postdiet 26.3±2.9 g, P<0.05).

Lipids and TAG content

Two lipid resonances were detected on *in vivo* spectra acquired from the midventricular septum as shown on Figure 1b. The prominent peak at 1.41 ppm was assigned to the methylene group and the weaker peak at 0.98 ppm was assigned to the terminal methyl group[24, 25]. Consistent with previous studies of mouse heart septum, the NMR signal from lipids was exclusive to the intracellular compartment with no evidence of extracellular lipids[18, 25].

Figure 3 displays lipid levels determined by MRS. Mobile lipid content of MHC-PPARα hearts was greater than in NTG, and HFD increased lipid content in both groups. The four experimental groups of pre- and post-diet NTG and MHC-PPARα displayed three different levels of mobile lipid content in the heart. But only at the highest of the three lipid contents, did principal strains change, as discussed below. Lipid content did not change over 2 weeks of RCD in either MHC-PPARα or NTG hearts.

Consistent with ^{1}H MRS of lipid, TAG content in separate groups of harvested for assay was also elevated in PPARα hearts at baseline versus NTG (Figure 4). While mobile lipids were elevated in both groups following HFD, TAG content in MHC-PPARα hearts harvested immediately after the post-HFD MRS/MRI study remained similar to TAG levels of the MHC-PPARα hearts harvested without HFD. Thus, despite increasing lipid content over two weeks of HFD, MHC-PPARα hearts contained similar TAG levels as did MHC-PPARα hearts not receiving HFD. These data suggest that the increased lipid content of MHC-PPARα at two weeks of HFD hearts was represented by changes in lipid species other than TAG, and that this ^{1}H MRS signal from lipid is neither solely attributable, nor exclusive to myocardial TAG content alone.

2-D Strains

Figure 5 displays 2-D principal E1 and E2 strains from both experimental groups before and after HFD in epi- and endo-cardial layers of the midventricular septum. Strains did not change after 2 weeks of RCD. There were no differences in epicardium and endocardium E1 and E2 between NTG and MHC-PPARα mice before HFD. After HFD, the biggest changes in both E1 and E2 strains appeared in the endocardial layer of MHC-PPARα hearts, whereas no significant change in either strain occurred in NTG. After HFD, endocardial E1 and E2 strains in MHC-PPARα hearts dropped by 30% and 25%, respectively, (P<0.05). Endocardial E1 and E2 in post-diet MHC-PPARα hearts were by 35% and 33% lower, respectively, than corresponding values in the post-diet NTG (P<0.05). While epicardial strains were reduced after HFD, only E1 dropped significantly (20% change, P<0.05).

Epicardial E2 strain in post-diet MHC-PPARα were 12% lower than E2 in post-diet NTG ($P<0.05$).

Interestingly, E1 and E2 both remained at control levels in pre-diet groups, despite elevated lipid content in the MHC- PPARα hearts, while the increased lipid resulting from HFD did not affect strain in NTG hearts. Not until lipid was elevated to a.u. values greater than 2.0, in the MHC-PPARα hearts, did strain values become affected by the diet (Figures 3 and 5). These data suggest that short term intramyocardial lipid accumulation does not impact 2D myocardial strains until a critical lipid content is established, as seen in the MHC- PPARα hearts after 2 weeks of high fat diet. As shown in Figure 6, a significant negative correlation exists between the endocardial values of E1 and lipid content for all hearts (before and after HF diet), as revealed by bivariate correlations (Pearson $r = -0.63$, $P<0.05$), but such correlation did not exist for E2 values.

These changes in principal 2-D strain mirror the response of more macroscopic changes in LV function, as indicated by the percent of wall thickening in the left ventricular. Figure 7 displays % WT values for both the septal region (Figure 7a) and averaged % WT over the whole LV wall (Figure 7b), that are consistent with previous MRI data for the in vivo mouse heart[26]. Notably, the data indicate a significant drop in %WT in the hearts of PPARα mice after only two weeks of HFD. Previously published echocardiographic measurements only indicate changes in fractional shortening in this low-overexpressing strain after four weeks of high fat diet[14]. Another study reports no impairment of contractile performance in isolated perfused hearts due to 2 weeks of HFD for either MHC-PPARα (404-4 line) or NTG mice[27].

DISCUSSION

This study provides the first demonstration of coincident changes in LV wall mechanics and intramyocardial lipid content, in response to short-term exposure to a high fat diet. While previous studies, both in humans and animals, have associated the eventual development of cardiomyopathy in hearts with alterations in fatty acid metabolism that produce increases in myocardial triacylglyceride, the current findings demonstrate that the 2-D strain values in the LV wall are compromised during the same time course of the elevated lipid contents. While previous investigations have shown that lipid accumulation in the myocardium predates global changes in LV function and the eventual development of cardiomyopathy, we present here the first data showing early changes in LV wall mechanics that coincide with initial increases in myocardial lipid in hearts that are susceptible to steatosis.

In contrast, normal hearts showed elevated lipid content after the brief high fat diet, but at levels significantly lower than PPARα hearts, and yet retained normal LV wall function. The increase in myocardial mobile lipids and TAG in NTG mice demonstrates that even a relatively short term exposure to chronic HFD induces cardiac lipid accumulation. While the modest elevation of lipid in both the PPARα hearts at baseline and the NTG hearts after the high fat diet did not affect 2-D strains, the heightened, post-diet lipid content induced in the PPARα mice was associated with impaired 2-D strains in the epi- and endocardial layers (Figure 5). Importantly, these results suggest an acute stepwise response of 2-D strain reduction to increasing lipid levels, below which no changes in LV wall mechanics were displayed.

As indicated in Figure 3, the high fat diet protocol produced three levels of myocardial lipid content among the experimental groups: the lowest lipid level occurred in the pre-diet NTG hearts, elevated lipid content was similarly detected in post-diet NTG hearts and pre-diet PPARα hearts, and the highest lipid content was induced in the post-diet PPARα hearts.

While the low and elevated lipid levels in both NTG and PPARα hearts was not associated with any contractile dysfunction, the highest lipid content, as observed in PPARα hearts following the high fat diet, was associated with significant reductions in both principal strains, E1 and E2 (Figure 5). The implication of this distinction among strain values of the experimental groups is that a critical level of intramyocardial lipid was reached in the post-diet hearts that produced changes in 2-D strains.

The predisposition of the low-overexpressing PPARα mouse heart for increased TAG content in response to high dietary fat is known to result in eventual contractile dysfunction, as shown by indices of LV function in the *in vivo* and ex vivo mouse heart, following four weeks of high fat diet[14]. Importantly, the authors also reported no evidence of fibrosis or apoptosis in the MHC-PPARα hearts after as much as 8 weeks of HFD. However, evidence of LV diastolic dysfunction and reduced fractional shortening was observed in this 404-4 line after 4 weeks of HFD. Recently published data from isolated perfused hearts of the same 404-4 line show no evidence of contractile dysfunction after 2 weeks of HFD[27].

In the current study, we observed no evidence of diastolic dysfunction after only two weeks of HFD (Figure 7c), despite reductions in 2-D strain (Figure 5) and in percentage of thickening of the LV (Figures 7a and 7b). The more pronounced response of 2-D strains in the endocardial layer than in the epicardium is finding consistent with the compromised mechanics of the LV wall in diseased hearts[28]. The present study does not distinguish whether the primary mechanism of reduced strain is either the direct action of lipotoxic intermediates or the purely mechanical influence of lipid droplet infiltration of the myocardium. However, the general effect of increased lipid content on transmural changes in principal strains in LV wall function can be interpreted as reduced tissue compliance, due to reduction in stretch and compression. These reduced changes may contribute to compromised LV wall thickening.

Interestingly, a recent MRS/MRI study in healthy humans[29] on effects of short term high-fat diet does not demonstrate changes in lipid content nor impaired function, and is thus consistent with our current observations of the cardiac response to short term high fat diet in the nontransgenic mice. Evidence of compromised LV wall function only occurred at the highest lipid level, that was induced in the hearts of the MHC-PPARα mice (Figures 3 and 5). Therefore, the use of principal 2-D strain measurements, and the specificity of the strain changes in the endocardial layer, may provide a more sensitive index for early changes in LV wall dynamics at elevated lipid levels.

After HFD, lipid content in the septum did not correlate with LV TAG content (Figure 8). Indeed, while both TAG and the MRS-observed lipid content increased in NTG hearts after HFD, the response of TAG and lipid values to HFD diverged in PPARα hearts. This divergence suggests that the elevation of lipid content in hearts predisposed to steatosis is not restricted solely to TAG. Therefore, we propose that the intramyocardial lipid signals detected by ^{1}H MRS in this particular study originate from a larger pool of mobile lipid, and not exclusively from TAG. Nonetheless, the key finding of this report remains that in response to a short term, high fat diet of two week, both the 2-D strains did not change with significant increases in the myocardial content of either total mobile lipid or TAG until a critical level of lipid content was reached.

METHODOLOGICAL CONSIDERATIONS AND STUDY LIMITATIONS

Systolic strains represent the measure of the myocardial deformation and thus represent and index of contractility within the chamber wall [30]. The strain tensor, as an index of

myocardial deformation, is induced by internal stress from active contractile elements and passive components due to the material properties.

Image guided, or localized, MRS is currently the only noninvasive modality that provides direct *in vivo* measurements of cardiac metabolites without exogenous tracers[31–34]. Several *in vivo* human MRS studies have examined impact of diet and health on myocardial lipid accumulation. Szczepaniak et al [15] reports that MRS detects cardiac triglyceride in the a 6 cc volume of myocardium in lean individuals, and provides valid and reproducible results with correlation to left ventricular volume, septal wall shortening and the individual's weight. In healthy persons, myocardial lipid levels have been positively correlated to body mass index [35] and myocardial triglyceride response was related to body mass index following a 48-hrs fast [36]. Work by McGavock et al [1] showed that lipid overstorage in human cardiac myocytes occurs early in impaired glucose tolerance and type 2 diabetes mellitus patients. However in the present study, comparison of mobile lipid content, via MRS, to TAG content, from biochemical assays of myocardium, indicates that the MRS signal from lipid is not exclusively attributable to TAG alone.

The our earlier study, applying tagging grids of 0.33 mm, has now enabled the current evaluation of transmural changes in 2-D principal strains in response to elevated myocardial lipid[12]. Thus, the combination of ultra-high field MRI and MRS offer a unique combination of high sensitivity, and high spectral and spatial resolution for longitudinal *in vivo* murine studies of cardiac function and metabolism [37].

CONCLUSIONS

This study examined the influence of moderate lipid accumulation in the myocardium on principal E1 and E2 strains in the left ventricular wall. Myocardial lipid and TAG levels were increased in hearts of normal and transgenic MHC-PPARα mice that exhibit low overexpression of PPARα. However, the elevated cardiac lipid content in MHC-PPARα mice after a high fat diet was not associated with further increases in triacylglyceride content.

This short term, high-fat diet induced cardiac lipid accumulation without immediate evidence of contractile dysfunction. However, at a critical level of elevated myocardial lipid, as displayed in MHC-PPARα mice fed the high fat diet, E1 and E2 strains were attenuated, with the most pronounced reductions in the endocardial layer. The negative consequences of a short term high fat diet on 2-D strains were only apparent in the MHC-PPARα hearts, suggesting an underlying pathophysiological or genetic requirement for cardiac steatosis in the development of LV dysfunction.

Acknowledgments

Dr. Daniel P. Kelly, Burnham Institute for Medical Research, Orlando FL, provided breeding stock for rederivation of MHC-PPARα mice.

SOURCES OF FUNDING

This study was supported by NIH grants R37HL49244 and R01HL62702 (E.D.L.).

References

1. McGavock JM, Lingvay I, Zib I, Tillery T, Salas N, Unger R, Levine BD, Raskin P, Victor RG, Szczepaniak LS. Cardiac Steatosis in Diabetes Mellitus. A ^{1}H-magnetc Resonance Spectroscopy Study. Circulation. 2007; 116:1170–1175. [PubMed: 17698735]

2. Schaffer JE. Lipotoxicity: when tissue overeat. Curr Opin Lipidol. 2003; 14:281–287. [PubMed: 12840659]
3. Sharma S, Adrogue JV, Golfman L, Uray I, Lemm J, Youker K, Noon GP, Frazier OH, Taegtmayer H. Intramyocardial lipid accumulation in the failing human heart resembles the lipotoxic rat heart. FASEB J. 2004; 18:1692–1700. [PubMed: 15522914]
4. Weinberg JM. Lipotoxicity. Kindney International. 2006; 70:1460–1566.
5. Finck BN, Lehman JJ, Leone TC, Welch MJ, Bennett MJ, Kovacs A, Han X, Gross RW, Kozak R, Lopaschuk GD, Kelly DP. The cardiac phenotype induced by PPARα overexpression mimics that caused by diabetes mellitus. J Clin Invest. 2002; 109:121–130. [PubMed: 11781357]
6. Christoffersen C, Bollano E, Lindegaard ML, Bartels ED, Goetze JP, Andersen CB, Nielsen LB. Cardiac lipid accumulation associated with diastolic dysfunction in obese mice. Endocrinology. 2003; 144:3483–3490. [PubMed: 12865329]
7. Ouwens DM, Boer C, Fodor M, de Galan P, Heine RJ, Maassen JA, Diamant M. Cardiac dysfunction induced by high-fat diet is associated with altered myocardial insulin signaling in rats. Diabetologia. 2005; 48:1229–1237. [PubMed: 15864533]
8. Ouwens DM, Diamant M, Fodor M, Habets DDJ, Pelsers MMAL, El Hasnaoui M, Dang ZC, van den Brom CE, Vlasblom R, Rietdijk A, Boer C, Coort SLM, Glatz JFC, Luiken JJFF. Cardiac contractile dysfunction in insulin-resistant rats fed a high-fat diet is associated with elevated CD36-mediated fatty acid uptake and esterification. Diabetologia. 2007; 50:1938–1948. [PubMed: 17639306]
9. Park TS, Hu Y, Noh HL, Drosatos K, Okajima K, Buchanan J, Tuinei J, Homma S, Jiang XC, Abel ED, Goldberg IJ. Ceramide is a cardiotoxin in lipotoxic cardiomyopathy. J Lipid Res. 2008; 49:2101–2112. [PubMed: 18515784]
10. Landeen LK, Dederko DA, Kondo CS, Hu BS, Aroonsakool N, Haga JH, Giles WR. Mechanism of the negative inotropic effects of sphingosine-1-phosphate on adult mouse ventricular myocytes. Am J Physiol Heart Circ Physiol. 2008; 294:H736–H749. [PubMed: 18024550]
11. Hexeberg S, Hessevik I, Hexeberg E. Intravenous lipid infusion results in myocardial lipid droplet acumulation combined with reduced myocardial performance in heparinized rabbits. Acta Physiol Scand. 1995; 153:159–168. [PubMed: 7778456]
12. Hankiewicz JH, Lewandowski ED. Improved Cardiac Tagging Resolution at Ultra-High Magnetic Field Elucidates Transmural Differences in Principal Strain in the Mouse Heart and Reduced Stretch in Dilated Cardiomyopathy. J Cardiovasc Magn Reson. 2007; 9:891–898. [PubMed: 18066749]
13. Barger PM, Kelly DP. PPAR Signaling in the Control of Cardiac Energy Metabolism. Trends Cardiovasc Med. 2000; 10:238–245. [PubMed: 11282301]
14. Finck BN, Han X, Courtois M, Aimond F, Nerbonne M, Kovacs A, Gross RW, Kelly DP. A critical role for PPARα-mediated lipotoxicity in the pathogenesis of diabetic cardiomyopathy: Modulation by dietary fat content. PNAS. 2003; 100:1226–1231. [PubMed: 12552126]
15. Szczepaniak LS, Dobbins RL, Metzger GJ, Sartoni-D'Ambrosia G, Arbique D, Vongpatansin W, Unger R, Victor RG. Myocardial Triglycerides and Systolic Function in Humans: In Vivo Evaluation by Localized Proton Spectroscopy and Cardiac Imaging. Magn Reson Med. 2003; 49:417–423. [PubMed: 12594743]
16. Iacobellis G, Leonetti F. Epicardial Adipose Tissue and Insulin Resistance in Obese Subjects. J Clin Endocrinol Metab. 2005; 90:6300–6302. [PubMed: 16091479]
17. Abel ED, Litwin SE, Sweeney G. Cardiac Remodeling in Obesity. Physiol Rev. 2008; 88:389–419. [PubMed: 18391168]
18. Lehman JJ, Boudina S, Hausler Banke N, Sambandam N, Han X, Young DM, Leone TC, Gross RW, Lewandowski ED, Abel ED, Kelly DP. The transcriptional coactivator PGC-1 is essential for maximal and efficient cardiac mitochondrial fatty acid oxidation and lipid homeostasis. Am J Physiol Heart Circ Physiol. 2008; 295:H185–H196. [PubMed: 18487436]
19. Liu W, Chen J, Ji S, Allen JD, Bayly PV, Wickline SA, Yu X. Harmonic phase magnetic resonance imaging tagging for direct quantification of Lagrangian strain in rat hearts after myocardial infraction. Magn Reson Med. 2004; 52:1282–1290. [PubMed: 15562486]

20. Amini, AA.; Prince, JL., editors. Measurement of Cardiac Deformations from MRI: Physical and Mathematical Models. Luwer Academic Publishments; Dordrecht, Netherlands: 2001.
21. Johansson C, Thorén P. The effects of triiodothyronine (T3) on heart rate, temperature and ECG measured with telemetry in freely moving mice. Acta Physiol Scand. 1997; 160:133–138. [PubMed: 9208039]
22. Wiesmann F, Neubauer S, Haase A, Hein L. Can we use vertical bore magnetic resonance scanners for murine cardiovascular phenotype characterization? Influence of upright body position on left ventricular hemodynamic in mice. J Cardivasc Magn Reson. 2001; 3:311–315.
23. Yang J-N, Tiselius C, Dare E, Johansson B, Valen G, Fredholm BB. Sex differences in mouse heart rate and body temperature in their regulation by adenosine A1 receptors. Acta Physiol. 2007; 190:63–75.
24. Ugurbil K, Petein M, Maidan R, Michurski S, Cohn JN, From AH. High resolution proton NMR studies of perfused rat hearts. FEBS. 1984; 167:173–78.
25. Schneider JE, Tyler DJ, ten Hove M, Sang AE, Cassidy PJ, Fischer A, Wallis J, Sebag-Montefiore LM, Watkins H, Isbrandt D, Clarke K, Neubauer S. In Vivo Cardiac ^{1}H-MRS in the Mouse. Magn Reson Med. 2004; 52:1029–1035. [PubMed: 15508174]
26. Yang Z, Berr SS, Gilson WD, Toufektsian M-C, French B. Simultaneous Evaluation of Infarct Size and Cardiac Function in Intact Mice by Contrast-Enhanced Cardiac Magnetic Resonance Imaging Reveals Contractile Dysfunction in Noninfarcted Regions Early After Myocardial Infarction. Circulation. 2003; 109:1161–1167. [PubMed: 14967719]
27. Hausler-Banke N, Wende AR, Leone TC, O'Donnell JM, Abel ED, Kelly DP, Lewandowski ED. Preferential Oxidation of Triacylglyceride-Derived Fatty Acids in Heart Is Augmented by the Nuclear Receptor PPARα. Circulation Research. 2010; 107:233–41. [PubMed: 20522803]
28. Hankiewicz JH, Goldspink PH, Buttrick PM, Lewandowski ED. Principal strain changes precede ventricular wall thinning during transition to heart failure in a mause model of dilated cardiomyopthy. Am J Physiol Heart Circ Physiol. 2008; 294:H330–H336. [PubMed: 17965277]
29. Lamb HJ, Smit JWA, van der Meer RW, Hammer S, Doornbos J, de Roos A, Romijnb JA. Metabolic MRI of myocardial and hepatic triglyceride content in response to nutritional interventions. Current Opinion in Clinical Nutrition and Metabolic Care. 2008; 11:573–579. [PubMed: 18685452]
30. McVeigh ER, Zerhouni EA. Noninvasive Measurement of Transmural Gradients in Myocardial Strain with MR Imaging. Radiology. 1999; 180:677–683. [PubMed: 1871278]
31. den Hollander JA, Evanochko WT, Pohost GM. Observation of cardiac lipids in humans by localized ^{1}H magnetic resonance spectroscopic imaging. Magn Reson Med. 1994; 32:175–180. [PubMed: 7968439]
32. Felblinger J, Jung B, Slotboom J, Boesch C, Kreis R. Methods and reproducibility of cardiac/respiratory double-triggered ^{1}H-MR spectroscopy of the human heart. Magn Reson Med. 1999; 42:903–910. [PubMed: 10542349]
33. Hudsmith LE, Neubauer S. Magnetic Resonance Spectroscopy in Myocardial Disease. J Am Coll Cardiol Img. 2009; 2:87–96.
34. Singhal A, Shivkumar K, Huda A, Thomas MA. Current status of cardiac MR spectroscopy. Progress in Nuclear Magnetic Resonance Spectroscopy. 2009; 54:255–277.
35. McGavock JM, Victor RG, Unger RH, Szczepaniak LS. Adiposity of the Heart, Revisited. Ann Interm Med. 2006; 144:517–524.
36. Reingold JS, McGavock JM, Kaka S, Tillery T, Victor RG, Szczepaniak LS. Determination of Triglyceride in the Human Myocardium by Magnetic Resonance Spectroscopy: Reproducibility and Sensitivity of the Method. Am J Physiol Endocrinol Metab. 2005; 289:E935–E939. [PubMed: 15972271]
37. Schneider, JE.; Neubauer, S. Applications in Medical and Pharmaceutical Sciences. Springer; Netherlands: 2006. Experimental Cardiovascular MR in Small Animals. in book Modern Magnetic Resonance, part 2; p. 835-853.

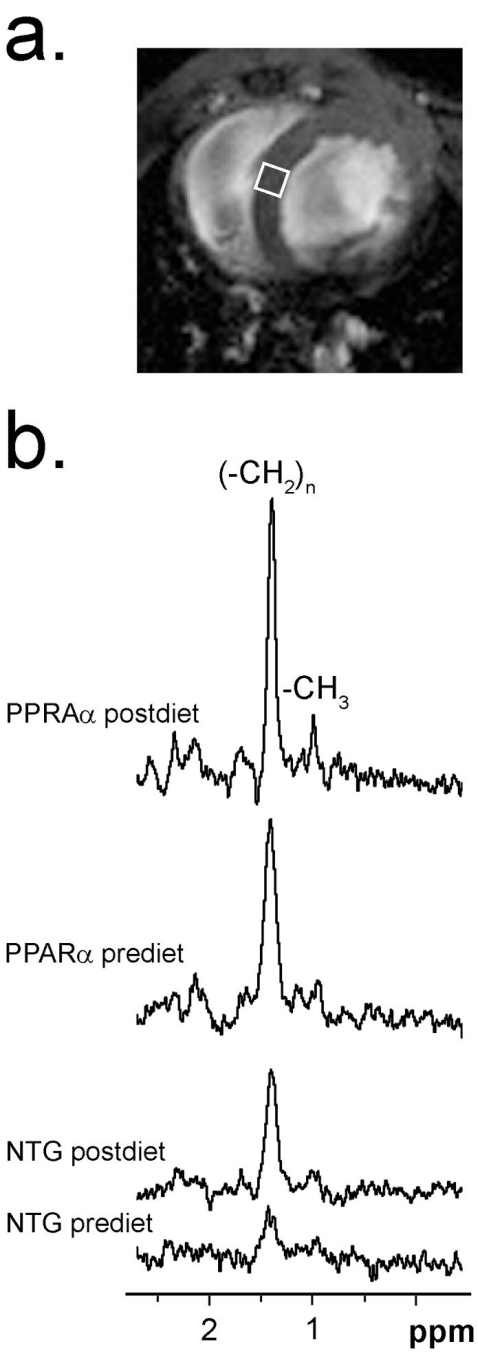

Figure 1.

^{1}H MRS of cardiac lipid. a) Scout image displaying 1×1×1 mm^{3} volume of interest (VOI) on midventricular septum for *in vivo* ^{1}H MRS. b) Typical water suppressed ^{1}H NMR spectra of intramyocardial lipid in pre-diet and post-diet NTG and MHC-PPARα hearts, showing resonance signal from acyl-chain methylene protons $(-CH_2)_n$ at 1.41 ppm. Weak signal at 0.98 ppm visible on MHC-PPARα spectra is from terminal methyl group protons $(-CH_3)$. Signal-to- noise; MHC-PPARα: pre-diet 19.5 and post-diet 29.9, NTG: prediet 5.3 and postdiet 14.6.

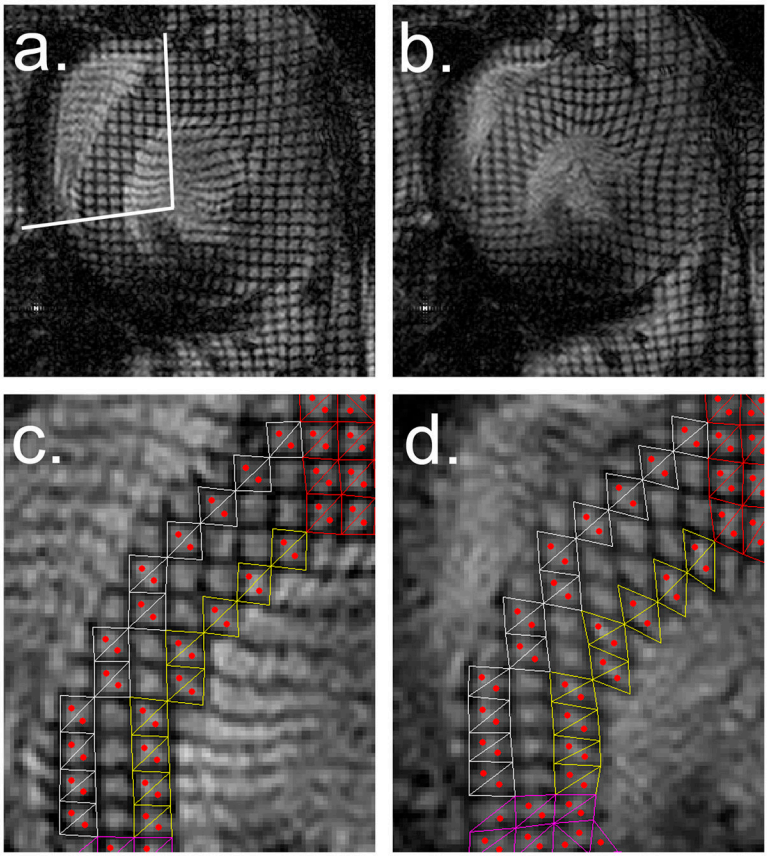

Figure 2.
Representative short-axis, tagged images (0.33×0.33 mm^2 grid with 0.1 mm grid line thickness) taken at: a) end-diastole (septal segment marked with white lines), b) end-systole. Zoomed images of septal segment shown at: c) end-diastole and d) end-systole, that display triangulated tagging elements for homogeneous strain measurement from tagged septum superimposed at epicardial (white) and endocardial layers (yellow). Centroids within triangles are marked in red. Note resolution of centroids across septal wall that enable separate analysis of epicardium and endocardium.

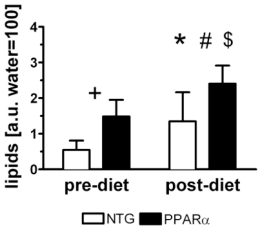

Figure 3.

Lipid content in hearts of MHC-PPARα and NTG mice increases after high fat diet. $^{+}$P<0.05, pre-diet MHC-PPARα vs. pre-diet NTG; *P<0.05, post-diet MHC-PPARα vs. post-diet NTG; $^{\#}$P<0.05, pre-diet MHC-PPARα vs. post-diet MHC-PPARα and $^{\$}$P<0.05, pre-diet NTG vs. post-diet NTG.

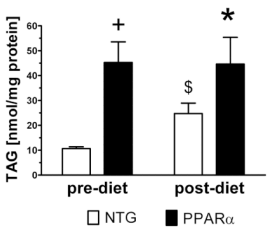

Figure 4.

Triacylglyceride content in 5 month old sub-group of MHC-PPARα and NTG mice not enrolled in HFD and in group of mice after 2 weeks HFD. Note that TAG content increased significantly for NTG and did not change for MHC-PPARα hearts. $^{\$}P<0.05$ pre-diet NTG vs. post-diet NTG, $^{+}P<0.05$ pre-diet MHC-PPARα vs. pre-diet NTG, *P<0.05 post-diet MHC-PPARα vs. post-diet NTG.

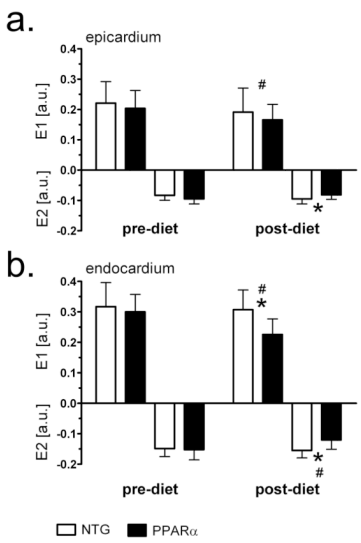

Figure 5.

Principal strains E1 and E2 before and after high-fat diet in midventricular septum of MHC-PPARα and NTG mice. a) epicardial values; b) endocardial values. Note reduced endocardial strains in MHC-PPARα hearts after high fat diet. * $P<0.05$, post-diet MHC-PPARα vs. post-diet NTG; # $P<0.05$, pre-diet MHC-PPARα vs. post-diet MHC-PPARα.

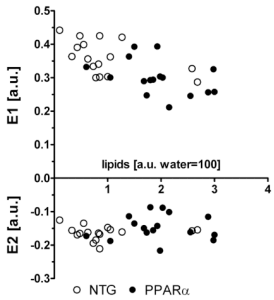

Figure 6.
Negative correlation exists between principal strains in endocardium and lipid content. Combined pre- and post- HFD data points show high correlation for E1: Pearson r = −0.63, P<0.05 and no correlation for E2: Pearson r = 0.18, P>0.05.

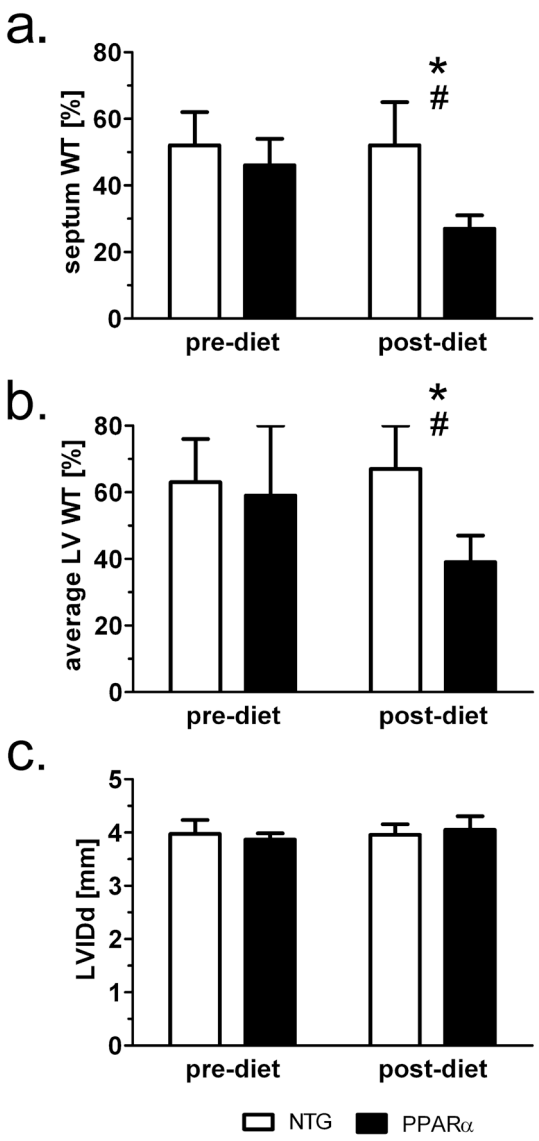

Figure 7.

Short term HFD induces systolic dysfunction in MHC-PPARα mice as seen on a percent wall thickening (%WT). a) %WT values from the septal region and b) averaged %WT from the four regions of the mid left ventricular wall: septum, lateral, anterior, and posterior. *P<0.05 post-diet MHC-PPARα vs. post-diet NTG; #P<0.05, pre-diet MHC-PPARα vs. post-diet MHC-PPARα. c) Short term HFD does not impair LV inner diameter at end-diastole (c).

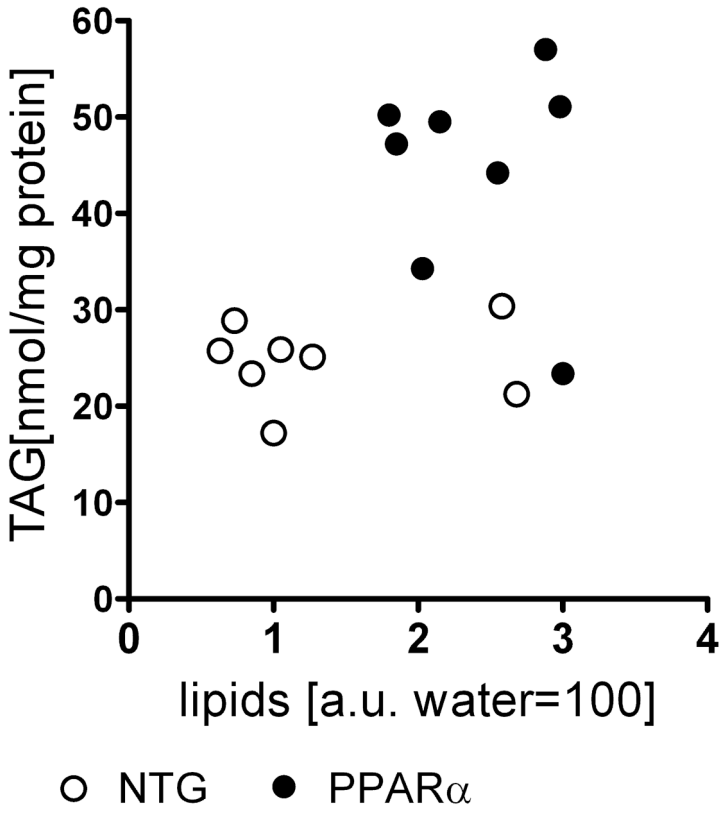

Figure 8.
Lipid content from MRS showed no correlation to triacylglyceride (TAG) assays of tissue samples in either group.